JOURNAL OF AIRCRAFT
Vol. 34, No. 6, November–December 1997

Dynamic Response of Composite Beams with Application to Aircraft Wings

S. H. R. Eslimy-Isfahany* and J. R. Banerjee†
City University, London EC1V 0HB, England, United Kingdom

In this paper, the response of composite beams to deterministic and random loads is investigated. Of particular interest is the inclusion of the (material) coupling between the bending and torsional deformation that usually exists because of the anisotropic nature of fibrous composites. First, the free vibration characteristics of a bending–torsion coupled composite beam are established using the basic governing differential equations of motion. The response problem is then formulated through the use of generalized coordinates and normal modes obtained from the free vibratory motion. The orthogonality condition of the bending–torsion coupled beam is derived to decouple the equations of motion. The overall response is then calculated by superimposing the response obtained in each mode. The developed theory is fairly general and can be applied to composite beams with any cross section, e.g., an aerofoil, as long as their rigidity and other properties are known. Numerical results are obtained for a cantilever composite aircraft wing with substantial coupling between bending and torsional modes of deformation. Both deterministic and random loads are considered in the analysis. The deterministic load is a harmonically varying concentrated flexural force at the tip, whereas the random load is that of an atmospheric turbulence, modeled by the von Kármán spectra, uniformly distributed over the length of the wing.

Introduction

RESEARCH interest in thin-walled composite beams has grown quite large in recent years. For instance, several authors have investigated the free vibration characteristics[1–7] of composite beams. However, comparatively very few authors have focused attention on the response characteristics.[8,9] This is because the response analysis of a structure is usually preceded by its free vibration analysis, particularly when the normal mode method is used. In this respect, the free vibration analysis of a composite beam is a basic step toward developing its forced vibration characteristics. However, it should be recognized that composite beams exhibit (material) coupling between various modes of deformation, e.g., bending–torsion coupling, unlike their metallic counterparts. This occurs mainly as a result of fiber orientations in laminated composites. Therefore, the response analysis of composite beams is somehow more complicated than that of metallic beams.

Abdelnaser and Singh[8] investigated the random vibration characteristics of cantilevered composite beams using third-order shear deformation theory. They obtained their solution by utilizing the eigenfunction of the free vibration problem and its adjoint. Their investigation shows that for thick composite beams, the effect of shear deformation on response can be significant. Rao and Ganesan,[9] on the other hand, studied the harmonic response of tapered composite beams using the finite element method. They presented results showing the influence of anisotropy, taper profile, and taper parameters for a wide range of composite beams.

This paper, however, uses an exact differential equation approach and addresses the coupled flexural–torsional response of composite beams to deterministic and random loads. Applications include aircraft wings and helicopter blades made of composite materials. This investigation stems from the authors' earlier work[10] on the response analysis of metallic beams for which the coupling between the bending and torsional deformation was caused by noncoincident mass axis (centroid) and elastic axis (shear center) of the beam. Thus, in the previous investigation,[10] the bending–torsion coupling effect was a consequence of the geometrical properties of the beam cross section rather than its material properties. In contrast, the bending–torsion coupling considered in this paper applies to composite beams because of the material properties of the beam. This type of material coupling occurs because of fiber orientations in laminated composites. The composite beam considered in this paper is assumed to be straight and uniform with a doubly symmetric cross section. It is made of thin-walled laminated plates, e.g., a flat or a box section composite beam. The bending–torsion (material) coupling effect, which is well known to occur for such composite beams, is quite fundamental to the consideration of this paper. The beam is subjected to a time-dependent bending and/or torsional load that can be either deterministic or random. Both concentrated and distributed loads for each of the previous two cases, i.e., deterministic and random, are considered when developing the theory. The deterministic load is assumed to vary harmonically, whereas in the case of random loading, the input is considered to be stationary and ergodic having a prescribed power spectral density (PSD) distribution. The response quantities considered in this paper are the flexural and torsional displacements at various points on the beam. The effects of shear deformation, rotatory inertia, and warping stiffness are considered to be small and neglected in the analysis.

The following steps are used when presenting the material of this paper. First, the natural frequencies and mode shapes of a bending–torsion coupled composite beam in free vibration are obtained using the method of Banerjee and Williams.[7] A normal mode method is then used to compute the frequency response function of the beam. (Note that linear small deflection theory has been used so that the overall response of the beam is represented by the superposition of all individual responses in each mode.) The Duhamel's integral is applied to calculate the response for the deterministic case. The evalua-

Received Feb. 15, 1996; presented as Paper 96-1411 at the AIAA/ASME/ASCE/AHS/ASC 37th Structures, Structural Dynamics, and Materials Conference, Salt Lake City, UT, April 15–17, 1996; revision received May 20, 1997; accepted for publication June 20, 1997.

*Research Student, Department of Mechanical Engineering and Aeronautics, Northampton Square.

†Senior Lecturer, Department of Mechanical Engineering and Aeronautics, Northampton Square. Member AIAA.

tion of the response for the random load is, however, carried out in the frequency domain by relating the PSD of the output to the PSD of the input, using the modulus of the complex frequency response function.

Finally, the theory developed in this paper is applied to a cantilever composite wing with substantial (material) coupling between bending and torsional modes of deformation. The effects of ply orientation on the rigidity properties of the wing and their subsequent effects on free and forced vibration characteristics are demonstrated by numerical results. However, note that the theory given in this paper (and, hence, the results), does not include time-dependent oscillatory unsteady aerodynamic forces that occur because of aerofoil motion.

Theory

The differential equations of motion of a viscously damped bending–torsion coupled composite beam (Fig. 1) are taken in the following form[3]:

$$EI\frac{\partial^4 u}{\partial y^4} + K\frac{\partial^3 \psi}{\partial y^3} + c_1\frac{\partial u}{\partial t} + m\frac{\partial^2 u}{\partial t^2} = f(y, t) \tag{1}$$

$$GJ\frac{\partial^2 \psi}{\partial y^2} + K\frac{\partial^3 u}{\partial y^3} - c_2\frac{\partial \psi}{\partial t} - I_\alpha\frac{\partial^2 \psi}{\partial t^2} = g(y, t) \tag{2}$$

where $u = u(y, t)$ and $\psi = \psi(y, t)$ are the transverse displacement and the torsional rotation of the reference axis (the reference axis is defined here as the locus of geometrical shear centers of the beam cross sections) of the beam, respectively; $f(y, t)$ and $g(y, t)$ are the external force and torque acting on and about the flexural axis of the beam, respectively; m is the mass per unit length; c_1 and c_2 are the linear viscous damping coefficients per unit length; EI, GJ, and K are, respectively, the bending, torsional, and bending–torsion coupling rigidities of the beam; I_α is the mass moment of inertia per unit length. (Note that the theory developed applies to more general cross sections, although the rectangular cross section is shown in Fig. 1 for convenience.)

Free Vibration Analysis

For undamped free vibration, the external load $f(y, t)$ and external torque $g(y, t)$ are set to zero together with the damping coefficients. The solutions are then assumed in the form

$$u(y, t) = U_n(y)e^{i\omega_n t} \tag{3}$$

$$\psi(y, t) = \Psi_n(y)e^{i\omega_n t} \tag{4}$$

where $n = 1, 2, 3, \ldots$ and $i = \sqrt{-1}$.

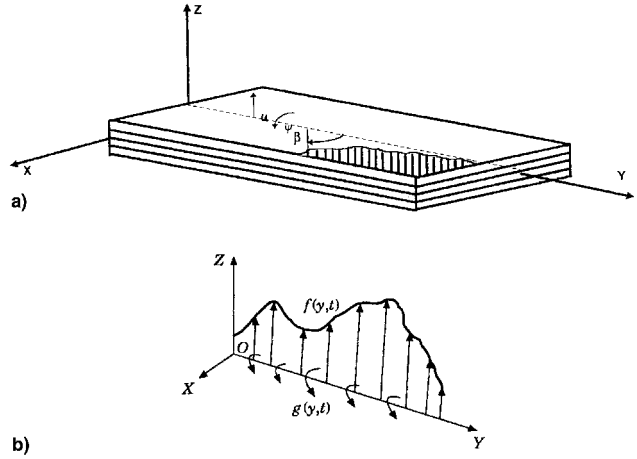

Fig. 1 a) Coordinate system and sign convention for positive ply angle of a laminated composite beam and b) the distribution of bending and torsional loads.

Substituting Eqs. (3) and (4) into Eqs. (1) and (2) gives the following two simultaneous differential equations for U_n and Ψ_n:

$$EI\frac{d^4 U_n}{dy^4} + K\frac{d^3 \Psi_n}{dy^3} - m\omega_n^2 U_n = 0 \tag{5}$$

$$GJ\frac{d^2 \Psi_n}{dy^2} + K\frac{d^3 U_n}{dy^3} + I_\alpha\omega_n^2 \Psi_n = 0 \tag{6}$$

Equations (5) and (6) can be combined into one equation by eliminating either Ψ_n or U_n, to give[7]

$$(D^6 + aD^4 - bD^2 - abc)W_n = 0 \tag{7}$$

where

$$W = U \text{ or } \Psi, \quad D = \frac{d}{d\xi}, \quad \xi = \frac{y}{L}, \quad a = \frac{\bar{a}}{c}, \quad b = \frac{\bar{b}}{c}, \quad c = 1 - \frac{K^2}{EIGJ} \tag{8}$$

with

$$\bar{a} = I_\alpha\omega_n^2 L^2/GJ, \qquad \bar{b} = m\omega_n^2 L^4/EI \tag{9}$$

and L is the length of the beam.

The solution of differential Eq. (7) is[7]

$$W_n(\xi) = D_1\cosh\alpha\xi + D_2\sinh\alpha\xi + D_3\cos\beta\xi + D_4\sin\beta\xi + D_5\cos\gamma\xi + D_6\sin\gamma\xi \tag{10}$$

where

$$\begin{aligned}\alpha &= [2(\varepsilon/3)^{0.5}\cos(\varsigma/3) - a/3]^{0.5}\\ \beta &= \{2(\varepsilon/3)^{0.5}\cos[(\pi - \varsigma)/3] + a/3\}^{0.5}\\ \gamma &= \{2(\varepsilon/3)^{0.5}\cos[(\pi + \varsigma)/3] + a/3\}^{0.5}\end{aligned} \tag{11}$$

in which

$$\begin{aligned}\varepsilon &= b + a^2/3\\ \varsigma &= \cos^{-1}[(27abc - 9ab - 2a^3)/2(a^2 + 3b)^{1.5}]\end{aligned} \tag{12}$$

In Eq. (7), a, b, and c are nondimensional quantities and are all positive[7] (note that[7,11] $0 < c < 1$).

Equation (10) represents the solution for both the bending displacement $U(\xi)$ and torsional rotation $\Psi(\xi)$. Thus,

$$\begin{aligned}U_n(\xi) &= A_1\cosh\alpha\xi + A_2\sinh\alpha\xi + A_3\cos\beta\xi + A_4\sin\beta\xi + A_5\cos\gamma\xi + A_6\sin\gamma\xi\\ \Psi_n(\xi) &= B_1\cosh\alpha\xi + B_2\sinh\alpha\xi + B_3\cos\beta\xi + B_4\sin\beta\xi + B_5\cos\gamma\xi + B_6\sin\gamma\xi\end{aligned} \tag{13}$$

where A_1–A_6 and B_1–B_6 are two different sets of constants that are not all independent. Substituting Eqs. (13) into Eqs. (5) and (6) shows that

$$\begin{aligned}B_1 &= (k_\alpha/L)A_2, \quad B_3 = (k_\beta/L)A_4, \quad B_5 = (k_\gamma/L)A_6\\ B_2 &= (k_\alpha/L)A_1, \quad B_4 = -(k_\beta/L)A_3, \quad B_6 = -(k_\gamma/L)A_5\end{aligned} \tag{14}$$

where

$$\begin{aligned}k_\alpha &= (\bar{b} - \alpha^4)/\bar{k}\alpha^3, \quad k_\beta = (\bar{b} - \beta^4)/\bar{k}\beta^3\\ k_\gamma &= (\bar{b} - \gamma^4)/\bar{k}\gamma^3, \quad \bar{k} = K/EI\end{aligned} \tag{15}$$

Equations (13), in conjunction with the boundary conditions, yield the eigenvalues (natural frequencies) and eigenfunctions (mode shapes) of a bending–torsional coupled composite beam. Based on Eqs. (5) and (6) and the boundary conditions, the following orthogonality condition is derived:

$$\int_0^L (mU_mU_n + I_\alpha \Psi_m \Psi_n)\,\mathrm{d}y = \mu_n \delta_{mn} \tag{16}$$

where μ_n is the generalized mass in the nth mode.

Response to Deterministic Loads

For a forced vibration problem, $u(y, t)$ and $\psi(y, t)$ can be expressed in terms of the eigenfunctions as follows:

$$u(y,t) = u(\xi L, t) = \sum_{n=1}^{\infty} q_n(t) U_n(y) \tag{17}$$

$$\psi(y,t) = \psi(\xi L, t) = \sum_{n=1}^{\infty} q_n(t) \Psi_n(y) \tag{18}$$

where $q_n(t)$ is the generalized time-dependent coordinate for each mode. Substituting Eqs. (17) and (18) into Eqs. (1) and (2), and using Eqs. (5) and (6), we obtain

$$\sum_{n=1}^{\infty} (m\omega_n^2 U_n q_n + c_1 U_n \dot{q}_n + m U_n \ddot{q}_n) = f(\xi, t) \tag{19}$$

$$\sum_{n=1}^{\infty} (-I_\alpha \omega_n^2 \Psi_n q_n - c_2 \Psi_n \dot{q}_n - I_\alpha \Psi_n \ddot{q}_n) = g(\xi, t) \tag{20}$$

where the overdot represents differentiation with respect to time.

Multiplying Eqs. (19) and (20) by U_m and $-\Psi_m$, respectively, then summing up these equations and integrating from 0 to L, and using the orthogonality condition of Eq. (16), gives the following equation:

$$\ddot{q}_n(t) + 2\zeta_n \omega_n \dot{q}_n(t) + \omega_n^2 q_n(t) = [F_n(t) + G_n(t)] \tag{21}$$

where $F_n(t)$ and $G_n(t)$ can be expressed as

$$F_n(t) = \frac{1}{\mu_n} \int_0^L U_n(y) f(y,t)\,\mathrm{d}y = \frac{1}{\mu_n} P_n(t) \tag{22a}$$

$$G_n(t) = -\frac{1}{\mu_n} \int_0^L \Psi_n(y) g(y,t)\,\mathrm{d}y = -\frac{1}{\mu_n} Q_n(t) \tag{22b}$$

$P_n(t)$ and $Q_n(t)$ in Eqs. (22) are the generalized forces, and ζ_n is the nondimensional damping coefficient in the nth mode given by

$$\int_0^L (c_1 U_m U_n + c_2 \Psi_m \Psi_n)\,\mathrm{d}y = 2\zeta_n \omega_n \mu_n \delta_{mn} \tag{23}$$

Using Duhamel's integral, the general solution for Eq. (21) can now be obtained as follows:

$$q_n(t) = e^{-\zeta_n \omega_n t}[A_n \cos(\omega_{nd} t) + B_n \sin(\omega_{nd} t)] + \frac{1}{\omega_{nd}} \int_0^t [F_n(\tau) + G_n(\tau)] e^{-\zeta_n \omega_n (t-\tau)} \sin[\omega_{nd}(t-\tau)]\,\mathrm{d}\tau \tag{24}$$

where $\omega_{nd} = \omega_n \sqrt{1-\zeta_n^2}$, and A_n and B_n are the coefficients related to the initial conditions. Finally, substituting Eq. (24) into Eqs. (17) and (18), the general solutions for $u(y, t)$ and $\psi(y, t)$ can be obtained as follows:

$$u(y,t) = \sum_{n=1}^{\infty} U_n(y) \left\{ e^{-\xi_n \omega_n t}[A_n \cos(\omega_{nd} t) + B_n \sin(\omega_{nd} t)] + \frac{1}{\omega_{nd}} \int_0^t [F_n(\tau) + G_n(\tau)] e^{-\zeta_n \omega_n (t-\tau)} \sin[\omega_{nd}(t-\tau)]\,\mathrm{d}\tau \right\} \tag{25}$$

$$\psi(y,t) = \sum_{n=1}^{\infty} \Psi_n(y) \left\{ e^{-\zeta_n \omega_n t}[A_n \cos(\omega_{nd} t) + B_n \sin(\omega_{nd} t)] + \frac{1}{\omega_{nd}} \int_0^t [F_n(\tau) + G_n(\tau)] e^{-\zeta_n \omega_n (t-\tau)} \sin[\omega_{nd}(t-\tau)]\,\mathrm{d}\tau \right\} \tag{26}$$

If the external force and torque are assumed as $f(y, t) = \delta(y - a_i) F_i \sin \Omega_i t$ and $g(y, t) = \delta(y - b_i) G_i \sin \Omega_i t$, which represent a system of concentrated simple harmonic forces and torques acting at points a_i and b_i, respectively, with $i = 1, 2, \ldots N$, and $\delta(y)$ is the Dirac delta function, then the dynamic response $u(y, t)$ and $\psi(y, t)$ can be obtained as

$$u(\xi,t) = \sum_{n=1}^{\infty} U_n(\xi) e^{-\zeta_n \omega_n t}[A_n \cos(\omega_{nd} t) + B_n \sin(\omega_{nd} t)] + \sum_{n=1}^{\infty} U_n(\xi) \sum_{i=1}^{N} \left\{ \frac{[U_n(a_i)F_i + \Psi_n(b_i)G_i]}{\mu_n[(\omega_n^2 - \Omega_i^2)^2 + (2\zeta_n \omega_n \Omega_i)^2]} \times [(\omega_n^2 - \Omega_i^2)\sin(\Omega_i t) - (2\zeta_n \omega_n \Omega_i)\cos(\Omega_i t)] \right\} \tag{27}$$

$$\psi(\xi,t) = \sum_{n=1}^{\infty} \Psi_n(\xi) e^{-\zeta_n \omega_n t}[A_n \cos(\omega_{nd} t) + B_n \sin(\omega_{nd} t)] + \sum_{n=1}^{\infty} \Psi_n(\xi) \sum_{i=1}^{N} \left\{ \frac{[U_n(a_i)F_i + \Psi_n(b_i)G_i]}{\mu_n[(\omega_n^2 - \Omega_i^2)^2 + (2\zeta_n \omega_n \Omega_i)^2]} \times [(\omega_n^2 - \Omega_i^2)\sin(\Omega_i t) - (2\zeta_n \omega_n \Omega_i)\cos(\Omega_i t)] \right\} \tag{28}$$

Equations (27) and (28) provide the general solutions for harmonically varying multipoint force and torque loading at given locations.

Response to Random Loads

The receptances $H_u(\xi, \xi_1, \Omega)$ and $H_\psi(\xi, \xi_1, \Omega)$ for the bending displacement u and the torsional rotation ψ, respectively, are defined by their amplitudes at the point ξ, when a harmonically varying force and/or torque with amplitude 1 and circular frequency Ω is applied at ξ_1. Thus, for the purpose of computing receptances, the externally applied loading $f(\xi, t)$ and $g(\xi, t)$ are represented by

$$f(\xi, t) = \delta(\xi - \xi_1) e^{i\Omega t} \qquad g(\xi, t) = \delta(\xi - \xi_1) e^{i\Omega t} \tag{29}$$

Substituting from Eqs. (29) into Eqs. (22) gives

$$F_n(t) = (1/\mu_n) U_n(\xi_1) e^{i\Omega t} \qquad G_n(t) = -(1/\mu_n) \Psi_n(\xi_1) e^{i\Omega t} \tag{30}$$

The solution of Eq. (21) for the previous loading is taken in the form

$$q_n(t) = q_{on} e^{i\Omega t} \tag{31}$$

Substituting Eq. (31) into Eq. (21) and using Eq. (30), we obtain

$$q_{on} = \frac{V_n(\xi_1)}{\mu_n(\omega_n^2 - \Omega^2 + 2i\zeta_n\Omega\omega_n)} \tag{32}$$

in which $V_n = a_F U_n(\xi_1) - a_G \Psi_n(\xi_1)$, where a_F (or a_G) is equal to 1 or 0, depending on whether applied transverse force (or torque) is presented or not. The receptance for u and ψ can now be obtained from Eqs. (17) and (18) with the help of Eq. (32), as follows:

$$H_u(\xi, \xi_1, \Omega) = \sum_n^{\infty} q_{on}(\xi_1, \Omega)U_n(\xi)$$
$$H_\psi(\xi, \xi_1, \Omega) = \sum_n^{\infty} q_{on}(\xi_1, \Omega)\Psi_n(\xi) \tag{33}$$

Once the receptance or the complex frequency response function is known, the response to a stationary, ergodic random load can be found by following the standard procedure.[12–14] (For determination of rigidity and other properties of composite beams required for the analysis, see Refs. 6, 15–17.)

The cross-spectral densities $S_f(\xi_1, \xi_2, \Omega)$ and $S_g(\xi_1, \xi_2, \Omega)$, and the cross-correlation functions $R_f(\xi_1, \xi_2, \Omega)$ and $R_g(\xi_1, \xi_2, \Omega)$ of the input excitation are related by their Fourier transform pair as

$$S_f(\xi_1, \xi_2, \Omega) = \frac{1}{2\pi}\int_{-\infty}^{\infty} R_f(\xi_1, \xi_2, \tau)e^{-i\Omega\tau}\,d\tau$$
$$R_f(\xi_1, \xi_2, \tau) = \int_{-\infty}^{\infty} S_f(\xi_1, \xi_2, \Omega)e^{i\Omega\tau}\,d\Omega$$
$$S_g(\xi_1, \xi_2, \Omega) = \frac{1}{2\pi}\int_{-\infty}^{\infty} R_g(\xi_1, \xi_2, \tau)e^{-i\Omega\tau}\,d\tau \tag{34}$$
$$R_g(\xi_1, \xi_2, \tau) = \int_{-\infty}^{\infty} S_g(\xi_1, \xi_2, \Omega)e^{i\Omega\tau}\,d\Omega$$

The cross-correlation functions $R_f(\xi_1, \xi_2, \tau)$ and $R_g(\xi_1, \xi_2, \tau)$ of the excitation are given by

$$R_f(\xi_1, \xi_2, \tau) = \langle f(\xi_1, t)f(\xi_2, t + \tau)\rangle \tag{35a}$$
$$R_g(\xi_1, \xi_2, \tau) = \langle g(\xi_1, t)g(\xi_2, t + \tau)\rangle \tag{35b}$$

where $\langle\ \rangle$ denotes the ensemble average of the stochastic process.

When the beam is acted upon by a finite number N of concentrated, randomly varying forces and torques, the spectral density function of the bending displacement and torsional rotation are related to the cross-spectral densities of the forces $S_f^{rs}(\Omega)$ and torques $S_g^{rs}(\Omega)$ as

$$S_u(\xi, \Omega) = \sum_{r=1}^{N}\sum_{s=1}^{N} H_u^*(\xi, \xi_r, \Omega)H_u(\xi, \xi_s, \Omega)[S_f^{rs}(\Omega) + S_g^{rs}(\Omega)]$$
$$S_\psi(\xi, \Omega) = \sum_{r=1}^{N}\sum_{s=1}^{N} H_\psi^*(\xi, \xi_r, \Omega)H_\psi(\xi, \xi_s, \Omega)[S_f^{rs}(\Omega) + S_g^{rs}(\Omega)] \tag{36}$$

where * denotes the complex conjugate.

For a distributed load, $S_f^{rs}(\Omega)$ and $S_g^{rs}(\Omega)$ are replaced by $S_f(\xi_1, \xi_2, \Omega)\,d\xi_1\,d\xi_2$, and $S_g(\xi_1, \xi_2, \Omega)\,d\xi_1\,d\xi_2$, and the summations are replaced by integrals over the whole beam. Thus, for a distributed load, the response spectral density is given by

$$S_u(\xi, \Omega) = \int_0^1\int_0^1 H_u^*(\xi, \xi_1, \Omega)H_u(\xi, \xi_2, \Omega)[S_f(\xi_1, \xi_2, \Omega) + S_g(\xi_1, \xi_2, \Omega)]\,d\xi_1\,d\xi_2$$
$$S_\psi(\xi, \Omega) = \int_0^1\int_0^1 H_\psi^*(\xi, \xi_1, \Omega)H_\psi(\xi, \xi_2, \Omega)[S_f(\xi_1, \xi_2, \Omega) + S_g(\xi_1, \xi_2, \Omega)]\,d\xi_1\,d\xi_2 \tag{37}$$

Substituting the receptance H_u and H_ψ from Eqs. (33) into (37), gives

$$S_u(\xi, \Omega) = \sum_m^{\infty}\sum_n^{\infty} d_m^*(\Omega)d_n(\Omega)\eta_{mn}(\Omega)U_m(\xi)U_n(\xi)$$
$$S_\psi(\xi, \Omega) = \sum_m^{\infty}\sum_n^{\infty} d_m^*(\Omega)d_n(\Omega)\eta_{mn}(\Omega)\Psi_m(\xi)\Psi_n(\xi) \tag{38}$$

where

$$d_n(\Omega) = 1/[\mu_n(\omega_n^2 - \Omega^2 + 2i\zeta\Omega\omega_n)] \tag{39}$$

$$\eta_{mn}(\Omega) = \int_0^1\int_0^1 V_m(\xi_1)V_n(\xi_2)[S_f(\xi_1, \xi_2, \Omega) + S_g(\xi_1, \xi_2, \Omega)]\,d\xi_1\,d\xi_2 \tag{40}$$

The mean square value of the response can now be found by integrating the spectral density functions over all frequencies, so that

$$\langle u^2(\xi, t)\rangle = \int_{-\infty}^{\infty} S_u(\xi, \Omega)\,d\Omega \tag{41}$$

$$\langle \psi^2(\xi, t)\rangle = \int_{-\infty}^{\infty} S_\psi(\xi, \Omega)\,d\Omega \tag{42}$$

If the input random excitation follows a Gaussian probability distribution, the response probability will also be Gaussian and, therefore, the response can be fully described by its spectral density function.

The preceding theory can be applied when the input random excitation is that of an atmospheric turbulence. The usually adopted PSD to model gust and atmospheric turbulence when obtaining the response of an aircraft wing is the well-known von Kármán spectra, given by[18]

$$S_f(\Omega) = \frac{\sigma_f^2 L_s}{\pi V}\frac{1 + (8/3)[1.339(L_s/V)\Omega]^2}{\{1 + [1.339(L_s/V)\Omega]^2\}^{11/16}} \tag{43}$$

where σ_f^2 is the mean square value of the gust (turbulence) velocity, L_s is the scale length of the turbulence, and V is the airspeed. The previous spectra will be used in obtaining the results of the illustrative example that follows.

Discussion of Results

The preceding theory is now applied to a graphite/epoxy composite wing.[19] The cross section of the wing is a thin-walled rectangular box (Fig. 2). This circumferentially asymmetric stiffness (CAS) configuration[19] exhibits bending–torsional coupling, because it has $(+\beta/+\beta)$ layup on the top wall, $(-\beta/-\beta)$ on the bottom wall, and $(+\beta/-\beta)$ on the sidewalls.

First, the bending EI, torsional GJ, and bending–torsional coupling K rigidities are established using the theory of Armanios and Badir.[6] The variations of these rigidities with ply angle are shown in Fig. 3.

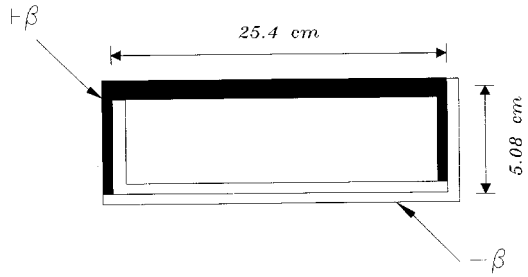

Fig. 2 Configuration of the laminated wing box section of Ref. 19 (ply angle β is measured from the *y* axis). Material = graphite/epoxy. $E_1 = 206.92 \times 10^9$ Nm^{-2}, $E_2 = E_3 = 5.17 \times 10^9$ Nm^{-2}, $G_{13} = G_{23} = 2.55 \times 10^9$ Nm^{-2}, $G_{12} = 3.10 \times 10^9$ Nm^{-2}, $\nu_{12} = \nu_{23} = \nu_{13} = 0.25$, and $\rho = 1529.48$ kgm^{-3}. Length = 203.2 cm and thickness = 1.016 cm.

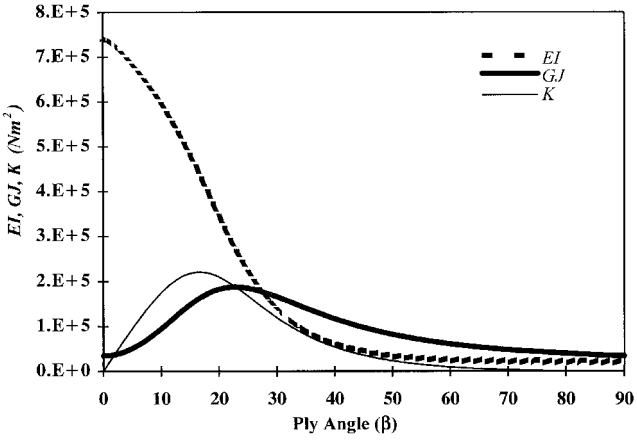

Fig. 3 Variation of *EI*, *GJ*, and *K* rigidities against ply angle.

Based on the preceding rigidities, the free vibration characteristics of the wing with cantilever end conditions are investigated for various ply angles, using the dynamic stiffness method.[7] The variation of the first five natural frequencies against ply angles are shown in Fig. 4. The effect of ply orientation on natural frequencies is quite pronounced. However, the essential purpose of Fig. 4 is to show trends and modal interchanges as a result of ply orientations that can be interpreted as follows. The first mode is basically a fundamental bending mode (with small amount of torsion in it), and it remains so for all ply angles. The second mode starts as a torsional mode in the $0 < \beta < 10$ region, and then becomes a bending-dominated mode. The variation of the third natural frequency reveals a different picture, it is predominantly a bending mode in the $0 < \beta < 10$ region; however, it becomes a predominantly torsional mode in the $10 < \beta < 25$ region and predominantly bending again in the $25 < \beta < 70$ region, before finally becoming a predominantly torsional mode again. In contrast, the fourth natural frequency first starts as a torsional mode within the $0 < \beta < 10$ range, then it becomes a bending-dominated mode within the $10 < \beta < 25$ range. Subsequently, it becomes torsion-dominated again within the $25 < \beta < 70$ range before finally becoming a bending mode. The modal interchange (flipover) between modes 3 and 4 around $\beta = 70$ deg is noticeable, i.e., the third bending mode becomes the first torsion, whereas the first torsion becomes the third bending mode. Finally, the fifth mode starts as a torsional mode and remains so until $\beta = 15$ deg, and then it becomes a bending mode within the $15 < \beta < 90$ range.

Representative results for the first five natural frequencies and mode shapes of the wing when $\beta = 10$ deg are shown in Fig. 5. Apart from the first mode (which has significant coupling between bending and torsion), the wing exhibits predominantly torsional deformation (Figs. 4 and 5). Note that the

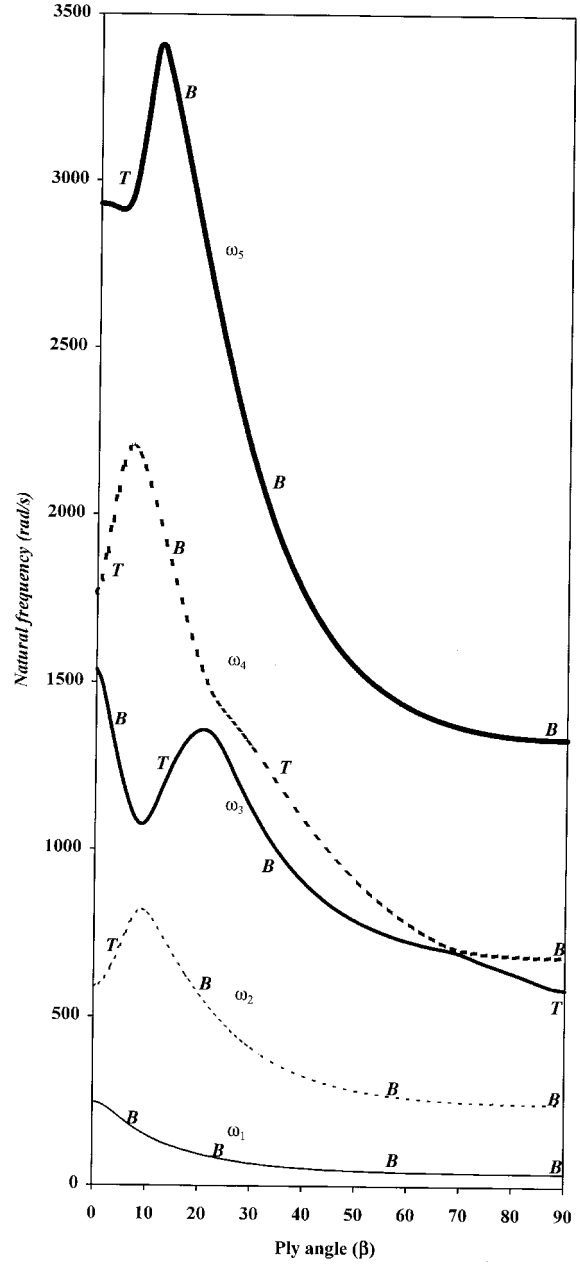

Fig. 4 Variation of the first five natural frequencies of the box wing against ply angle. *B*, bending and *T*, torsional.

first five modes of the wing were used in the response analysis for both deterministic and random loads and were subsequently found to be adequate. Damping was assumed to be 3% in all modes, i.e., $\zeta_n = 0.03$.

The amplitudes of the dynamic flexural and torsional displacements at the tip of the wing, under the action of a harmonically varying concentrated flexural force of unit amplitude at the tip, are computed using the present theory. The results for $\beta = 10$ deg are shown in Fig. 6, where the absolute values of the response are shown. The peaks in Fig. 6 correspond to the natural frequencies of the wing. For instance, the first peak occurs around the first natural frequency, i.e., 149 rad/s, whereas the second and third peaks occur around the second and third natural frequencies, i.e., 811, 1089 rad/s (Figs. 5 and 6). Note that the results shown in Fig. 6 are obtained under the action of flexural load only, but a dynamic torsional rotation is evident as a consequence of the (material) coupling effect. Because of the intrinsic nature of the material coupling present in laminated (fibrous) composites, the two

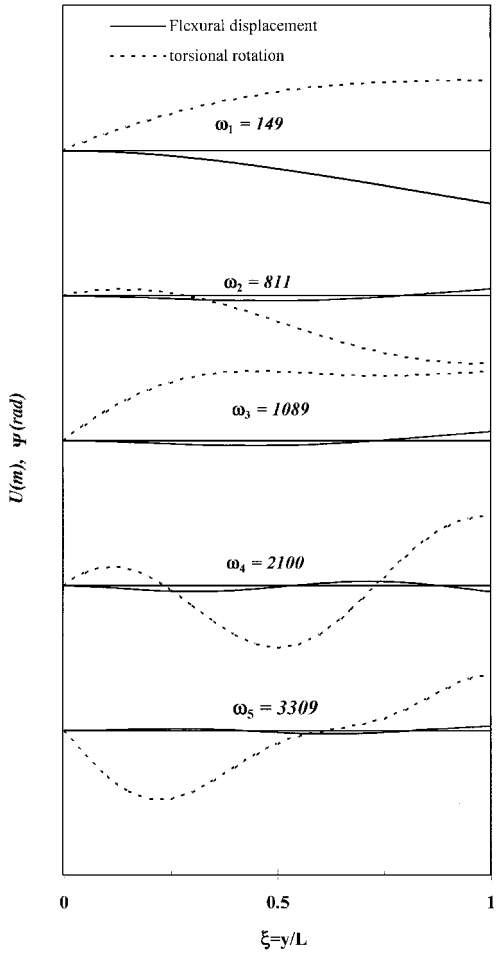

Fig. 5 Coupled bending–torsion natural frequencies (rad/s) and mode shapes of the box wing of Ref. 19 (β = 10).

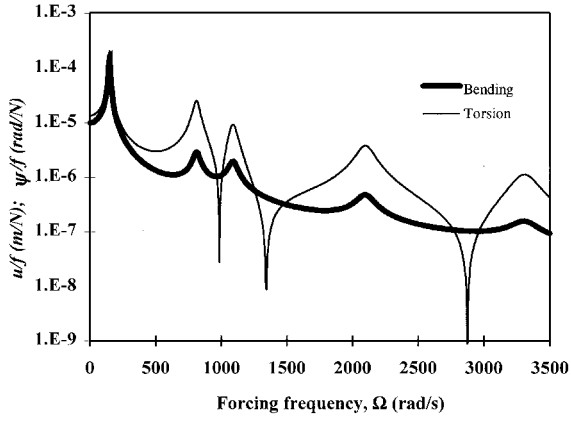

Fig. 6 Dynamic flexural and torsional response of the box wing of Ref. 19 because of a unit harmonically varying concentrated force at the tip (β = 10).

displacements, i.e., bending and torsion, must not be considered in isolation. At the tip where there is a concentrated flexural load (but no torsional load), the amplitude of the flexural response (unlike the torsional one) is always in the same direction as the applied load. However, for certain forcing frequencies, sudden drops in the torsional response occur as shown (in the logarithmic scale) in Fig. 6. This indicates a change in sign for the torsional rotation induced by flexural displacement.

Next, the flexural and torsional response of the wing caused by a uniformly distributed atmospheric turbulence modeled by the von Kármán spectra[18] see [Eq. (43)], is investigated. The spectrum is shown in Fig. 7 for three different values of L_s/V ratio. Again, the excitation is assumed to be flexural only, i.e., there is no externally applied torsional load on the wing. The mean square values of the bending displacements and torsional rotations against ply angle β are shown in Figs. 8a and 8b, respectively, for two different values of L_s/V ratio. As evident from these figures, the torsional response arises solely from bending–torsion (material) coupling. Because the bending rigidity reduces with the increase in ply angle (Fig. 3), the flexural response increases as a consequence. However, no such predictable pattern can be observed for the (flexure-induced) torsional response that has been computed in the absence of any externally applied torsional load. The authors' investigation has shown that the flexure-induced torsional response is quite a complex phenomenon, which is primarily dependent upon the bending–torsion coupling rigidity. Finally, the flexural and torsional responses were computed at various points on the wing. The mean square values of the flexural displacement and torsional rotation along the length of the wing for β

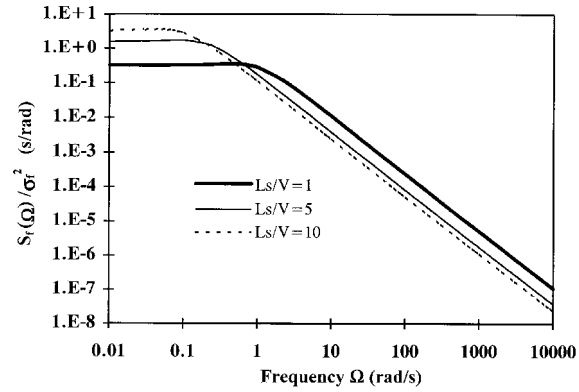

Fig. 7 Von Kármán PSD function for different L_s/V.

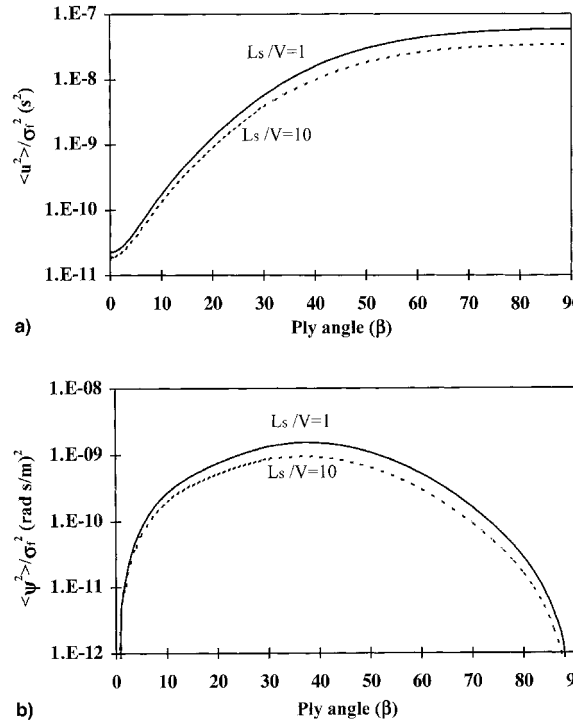

Fig. 8 Variation of mean square value of the a) flexural and b) torsional response of the box wing of Ref. 19 at the tip, against ply angle for different L_s/V ratios (ζ = 0.03).

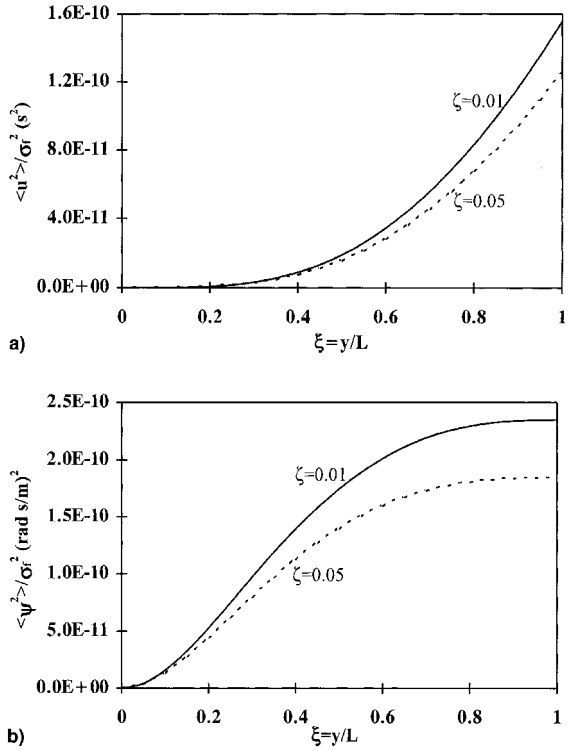

Fig. 9 Variation of mean-square value of the a) flexural and b) torsional response along the box wing of Ref. 19 for different damping coefficients (L_s/V = 10).

= 10 deg are shown in Figs. 9a and 9b, respectively, for two values of the damping ratio. Both flexural and torsional responses are maximum at the tip.

Conclusions

A theory has been developed to perform the response analysis of a bending–torsion materially coupled composite beam when subjected to deterministic or random loads. Applications include composite wings, for which flexural and torsional motions are coupled as a result of the intrinsic nature of laminated (fibrous) composites. Numerical results are given and discussed for a cantilever composite wing subjected to both deterministic and random loads.

The effects of ply orientation on rigidity properties and their subsequent effects on response characteristics are demonstrated. The investigation has shown that response induced by material coupling as a consequence of ply orientation can be significant.

Acknowledgment

The authors are grateful to the Ministry of Culture and Higher Education of Iran for providing the first author with a scholarship to carry out this research.

References

[1]Suresh, J. K., Venkatesan, C., and Ramamurti, V., "Structural Dynamic Analysis of Composite Beams," *Journal of Sound and Vibration*, Vol. 143, No. 3, 1990, pp. 503–519.

[2]Hodges, D. H., Atilgan, A. R., Fulton, M. V., and Rehfield, L. W., "Free Vibration Analysis of Composite Beams," *Journal of the American Helicopter Society*, Vol. 36, No. 3, 1991, pp. 23–35.

[3]Wu, X. X., and Sun, C. T., "Vibration Analysis of Laminated Composite Thin-Walled Beams Using Finite Elements," *AIAA Journal*, Vol. 29, No. 5, 1991, pp. 736–742.

[4]Chandrashekhara, K., and Bangera, K. M., "Free Vibration of Composite Beams Using a Refined Shear Flexible Beam Element," *Computers and Structures*, Vol. 43, No. 4, 1992, pp. 719–727.

[5]Teboub, Y., and Hajela, P., "Free Vibration of Generally Layered Composite Beams Using Symbolic Computations," *Composite Structures*, Vol. 33, No. 3, 1995, pp. 123–134.

[6]Armanios, E. A., and Badir, A. M., "Free Vibration Analysis of Anisotropic Thin-Walled Closed-Section Beams," *AIAA Journal*, Vol. 33, No. 10, 1995, pp. 1905–1910.

[7]Banerjee, J. R., and Williams, F. W., "Free Vibration of Composite Beams—An Exact Method Using Symbolic Computation," *Journal of Aircraft*, Vol. 32, No. 3, 1995, pp. 636–642.

[8]Abdelnaser, A. S., and Singh, M. P., "Random Vibration of Cantilevered Composite Beams with Torsion-Bending Coupling," *Probabilistic Engineering Mechanics*, Vol. 8, 1993, pp. 143–151.

[9]Rao, S. R., and Ganesan, N., "Dynamic Response of Tapered Beams Using Higher Order Shear Deformation Theory," *Journal of Sound and Vibration*, Vol. 187, No. 5, 1995, pp. 737–756.

[10]Eslimy-Isfahany, S. H. R, Banerjee, J. R., and Sobey, A. J., "Response of a Bending-Torsion Coupled Beam to Deterministic and Random Loads," *Journal of Sound and Vibration*, Vol. 195, No. 2, 1996, pp. 267–283.

[11]Weisshaar, T. A., and Foist, B. L., "Vibration Tailoring of Advanced Composite Lifting Surface," *Journal of Aircraft*, Vol. 22, No. 2, 1985, pp. 141–147.

[12]Crandall, S. H., and Mark, W. D., *Random Vibration in Mechanical System*, Academic, New York, 1963.

[13]Lin, Y. K., *Probabilistic Theory of Structural Dynamics*, McGraw–Hill, New York, 1967.

[14]Newland, D. E., *An Introduction to Random Vibration and Spectral Analysis*, Longman, London, 1984.

[15]Berdichevsky, V., Armanios, E., and Badir, A., "Theory of Anisotropic Thin-Walled Closed-Cross-Section Beams," *Composite Engineering*, Vol. 2, Nos. 5–7, 1992, pp. 411–432.

[16]Chandra, R., Stemple, A. D., and Chopra, I., "Thin-Walled Composite Beams Under Bending, Torsional and Extensional Loads," *Journal of Aircraft*, Vol. 27, No. 7, 1990, pp. 619–626.

[17]Minguet, P., and Dugundji, J., "Experiments and Analysis for Composite Blades Under Large Deflection, Part I: Static Behaviour, Part II: Dynamic Behaviour," *AIAA Journal*, Vol. 28, No. 9, 1990, pp. 1573–1588.

[18]Houbolt, J. C., Steiner, R., and Pratt, K. G., "Dynamic Response of Airplanes to Atmospheric Turbulence Including Flight Data on Input Response," NASA TR-R 199, June 1964.

[19]Cesnik, C. E. S., Hodges, D. H., and Patil, M. J., "Aeroelastic Analysis of Composite Wings," *Proceedings of the AIAA 37th Structural, Structural Dynamics, and Materials Conference*, AIAA, Reston, VA, 1996, pp. 1113–1123.